On the Use of Measured Vibration for Detecting Bridge Damage

Sreenivas Alampalli, Gongkang Fu, and Everett W. Dillon, *New York State Department of Transportation*

Bridge condition monitoring using modal properties, which has been suggested and studied recently, is perceived to supplement or even replace current inspection practice. However, its applicability is still unclear. A study conducted on a fracture-critical bridge, supplementing earlier studies on a scaled model bridge, is presented. The detectability of damage using measured vibration is addressed. Results indicate that modal frequencies can be used to detect the existence of damage or deterioration simulated here. However, the damage location cannot be identified with high confidence using mode shapes and their derivatives because damage affects mode shapes comparably at both damaged and undamaged locations.

Many highway bridges in the United States are structurally deficient or functionally obsolete. Periodic inspection has become a major part of maintaining the safety of these bridges, so that potentially hazardous conditions can be identified early enough to prevent serious consequences. Currently, FHWA requires every bridge be inspected at least every 2 years (*1*), but some deficiencies may develop and cause serious failure between inspections. The near failure of a viaduct in Rhode Island (*2*) and other recent bridge failures in several states (*3*) prompted researchers to look for new inspection tools. It is believed that remote bridge monitoring systems based on measured structural vibration will be helpful in bridge inspection in the future. It is well-known that modal frequencies and mode shapes will change with altered structural condition. Theoretically, the monitoring of these modal properties may be used for bridge diagnosis. The technique is commonly referred to as experimental modal analysis, modal testing, or dynamic monitoring.

Modal testing (*4*) recently received intensive attention because of the availability of Fourier analyzers, which instantaneously perform fast Fourier transforms. Several researchers have investigated changes in modal parameters due to simulated damages using laboratory bridge models and field bridges (*5–8*). Great efforts have been made to correlate measured modal parameters with simulated damages. Yet little attention has been paid to the sensitivity of modal parameters to common damage or deterioration of interest, which is critical in real-world application to bridge inspection. The major issue is that modal testing, like other experimental techniques, produces variable results when repeated, because of inevitable noise attributable to such causes as environment, electrical disturbance, and operators. This variation may be higher than the changes in modal parameters due to damage or deterioration, resulting in incorrect diagnosis.

This paper presents partial results of a study to examine the sensitivity of modal parameters in detecting fatigue cracks using frequencies, damping ratios, mode

shapes, and their derivatives. Modal tests were conducted on a 1/6 scale model of a multiple-steel-girder simple-span bridge including both intact and damaged states. Sensitivity of the modal parameters to changes of structural condition were studied using statistical methods. Results indicated that modal frequencies can be used in conjunction with mode shapes to identify the existence of commonly observed fatigue-related damages in steel highway bridges (*9*). However, it is difficult to identify damage locations using these modal parameters. The work described here was aimed at supplementing and verifying the previous laboratory work by conducting tests on a fracture-critical bridge and using commercially available modal-testing instrumentation and the latest analytical techniques for diagnosis of simulated damage.

Structure and Instrumentation

A fracture-critical bridge with two steel girders of 6.76-m span was the test structure. Located over Mud Creek on Van Duesen Road in Claverack, New York, the bridge was built in 1930 and was closed to service in 1988. It had two W18×64 steel beams supporting floor beams and a reinforced concrete deck, as shown in Figure 1. Its floor beams were fastened to the main beams by bolts. The main beams appeared to be embedded in the concrete abutments at both ends. A total of 54 data points were chosen, as shown in Figure 2, for modal testing measurements. (For practical applications, measurement points or sensor locations may have to be determined by considering expected damage or instrumentation costs.)

The general test setup is shown in Figure 3. It consisted of an impact hammer, a dynamic signal analyzer, signal conditioners, a stationary accelerometer, and a microcomputer. An impulse force hammer, PCB Model 086B50, with a plastic tip was used to excite the test structure, and the excitation induced was measured using a PCB load cell (with sensitivity of 10 mV/lbf) attached to the hammer tip. Acceleration responses of the structure were measured using PCB accelerometers (Flexcel Model 336A04 with 100 mV/g sensitivity). The accelerometers were fixed to the structure using magnets supplied by PCB Peizotronics. A dynamic signal analyzer (Tektronix Model 2630) obtained time domain data, transfer functions, power spectra, and coherence functions (*4*).

The locations of the data points (Figure 2) for obtaining transfer functions were chosen to represent the behavior of the structure for the modes of interest (0–200 Hz). Only the vertical vibration response perpen-

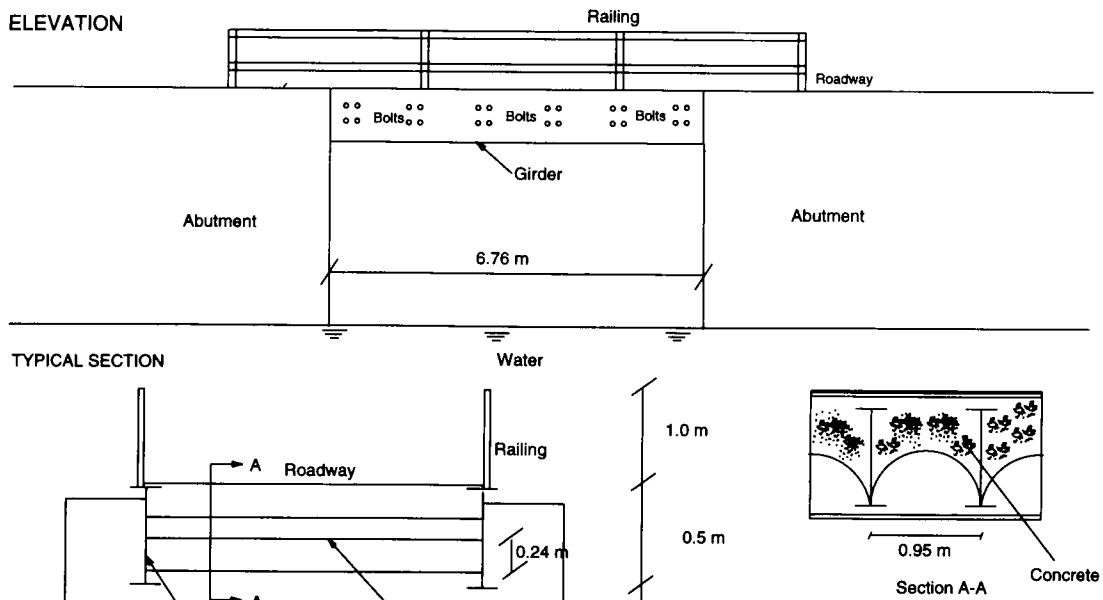

FIGURE 1 Test bridge (not to scale).

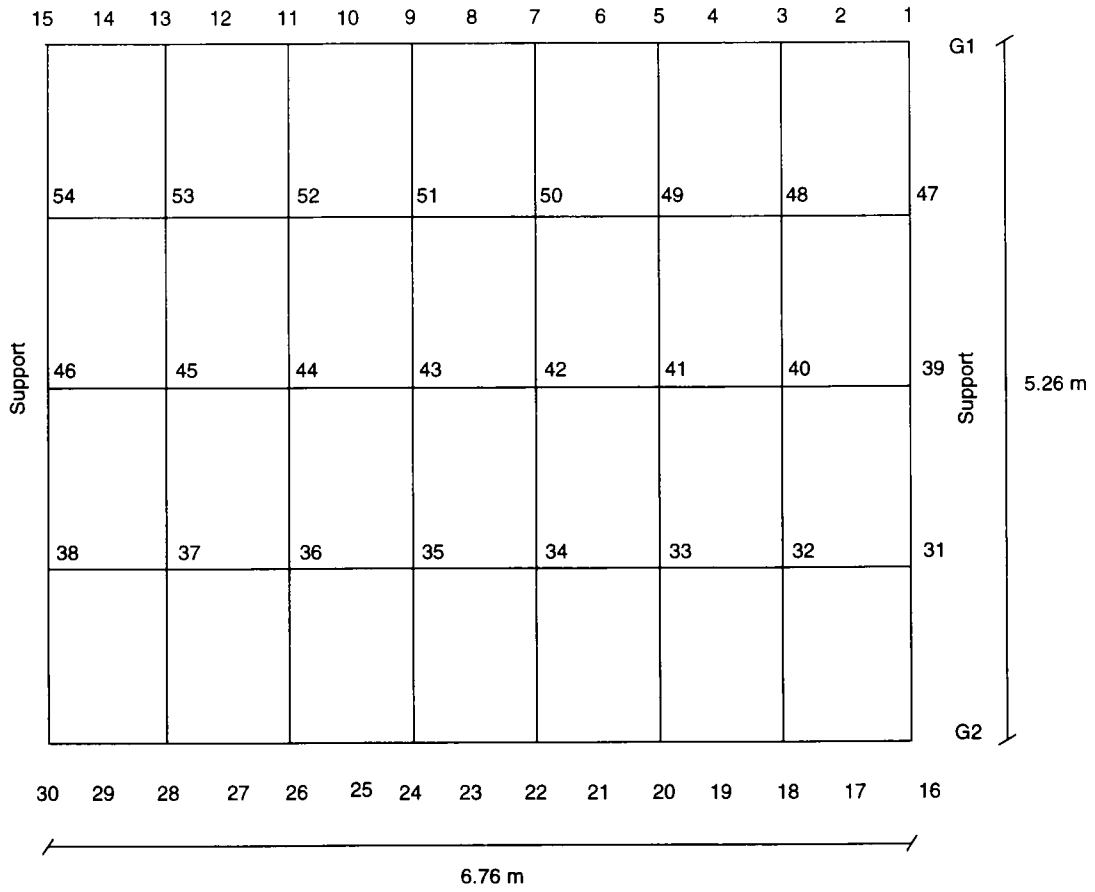

FIGURE 2 Data measurement points on test bridge.

dicular to the plane of the concrete deck was measured. The excitation input was given by the hammer at every data point shown in Figure 2, and the frequency response function (FRF) was obtained by measuring force input (of the impact hammer) and the response output of a stationary accelerometer at Point 27 (Figure 2). This location was chosen such that it was perceived and later verified not to be a modal node (i.e., a point theoretically having no motion for the mode) within the frequency range of interest. For each test, this procedure was repeated several times for the same point, and an average of FRFs was then stored with observation of good coherence. The coherence function indicated the consistency of the obtained data: 1.0 for perfect consistency and 0 for no consistency. For all the data collected, almost perfect coherence values (greater than 0.95) were recorded in the frequency range of interest. Reciprocity was also confirmed at the beginning of the test program by comparing FRFs with interchanged input and output locations. The required analyses were performed using software developed by Structural Measurement Systems, Inc., of San Jose, California, to obtain modal frequencies, modal damping values, and mode shapes.

Structural Signatures and Test Program

Candidates of Structural Signature

The following structural signatures were used for damage detection on the basis of their measured values: modal frequencies, modal damping ratios, mode shapes, modal assurance criterion factors (MAC), and coordinate modal assurance criterion factors (COMAC). The first three are inherent modal parameters of the structure, and the other two are derived from mode shapes

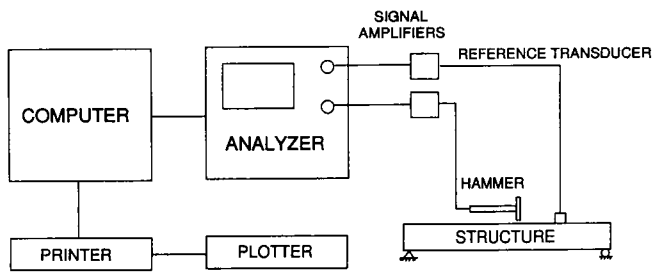

FIGURE 3 General test setup for impact hammer test.

as inherent structural indexes (*10,11*). Their intended functions in damage detection are discussed next.

MAC indicates correlation between two measured mode shapes from two different tests. Let $[\phi_A]$ and $[\phi_B]$ be the first and second sets of measured mode shapes in matrices form of sizes $n \times m_A$ and $n \times m_B$, respectively, where m_A and m_B are the number of modes in the respective sets and n is the number of coordinates (or number of data points) included. MAC is then defined for Modes j and k as follows:

$$\text{MAC}(j,k) = \left| \sum_{i=1,2,\ldots n} {}_i\{\phi_A\}_j \, {}_i\{\phi_B\}_k \right|^2 \div \left[\left(\sum_{i=1,2,\ldots n} {}_i\{\phi_A\}_j \, {}_i\{\phi_A\}_j \times \sum_{i=1,2,\ldots n} {}_i\{\phi_B\}_k \, {}_i\{\phi_B\}_k \right) \right]$$

$$j = 1, 2, \ldots, m_A \text{ and}$$

$$k = 1, 2, \ldots, m_B \qquad (1)$$

where ${}_i\{\phi_A\}_j$ is the ith coordinate of the jth column (mode) of $[\phi_A]$, and ${}_i\{\phi_B\}_k$ is the ith coordinate of the kth column (mode) of $[\phi_B]$.

MAC indicates the degree of correlation between the jth mode of the first set and the kth mode of the second set. MAC values vary from 0 to 1, with 0 for no correlation and 1 for full correlation. If Eigen vectors $\{\phi_A\}_j$ and $\{\phi_B\}_k$ are identical (e.g., for the same mode), Equation 1 will be unity indicating full correlation. Theoretically, mode shapes are invariable if the structure is not altered. Thus, MAC was used in this study to detect the existence of damage by identifying MAC values altered from their original values near 1 for individual modes.

COMAC is intended to identify locations where mode shapes from two sets of test data do not agree, indicating damage locations. For Location i and including L modes, COMAC is defined as

$$\text{COMAC}(i) = \left[\sum_{j=1,2,\ldots L} \left| {}_i\{\phi_A\}_j \, {}_i\{\phi_B\}_j \right| \right]^2 \div \left[\sum_{j=1,2,\ldots L} {}_i\{\phi_A\}_j^2 \sum_{k=1,2,\ldots L} {}_i\{\phi_B\}_k^2 \right] \qquad (2)$$

where the summation is carried out over L modes and ${}_i\{\phi_A\}_j$ and ${}_i\{\phi_B\}_j$ are the jth mode shapes at Point i from Tests A and B, respectively. Note that if $[\phi_A]$ and $[\phi_B]$ are identical, COMAC for all the measurement points will theoretically be unity, indicating no difference (damage) between the results of Tests A and B.

Random Variation of Measured Structural Signatures

Practically, instrumentation systems possess only certain degrees of accuracy, test environments may add noise to measured physical quantities, and required manual operations may also introduce fluctuation to test results. Identifying and quantifying such variation are necessary for practical applications. Ten impact tests were conducted between October 28, 1992, and November 6, 1993, to understand and evaluate variation in measured modal parameters in the field. The data were obtained using a 0–200 Hz base band, with a 0.125 Hz frequency resolution. The exponential window was used on the vibration response, and the force window was used on the hammer excitation. The mode shapes are shown in Figure 4. Tables 1 and 2 contain means, standard deviations (STD in Table 1), and coefficients of variation (COV) of the obtained modal parameters. MAC and COMAC values were calculated with the first set of test data as reference.

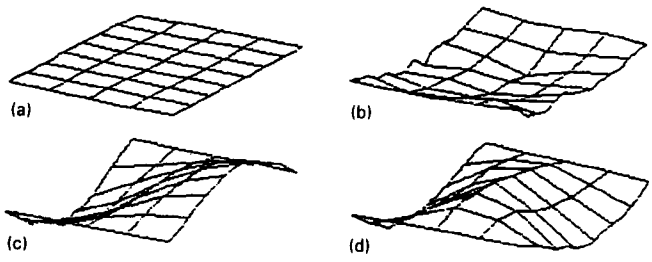

FIGURE 4 Mode shapes of test bridge: (*a*) undeformed, (*b*) Mode 1, (*c*) Mode 2, and (*d*) Mode 3.

TABLE 1 Random Variation of Measured Modal Parameters and MAC

	Modal Frequencies (Hz)		
	Mode 1	Mode 2	Mode 3
Mean	10.895	20.212	36.792
STD	.03740	.05313	.08588
COV (%)	.34326	.26288	.23343
	Modal Damping Ratios (%)		
	Mode 1	Mode 2	Mode 3
Mean	3.034	2.762	2.386
STD	0.301	0.140	0.176
COV (%)	9.921	5.069	7.376
	MAC Factors (with first data set as reference)		
	Mode 1	Mode 2	Mode 3
Mean	0.848	0.976	0.963
STD	0.025	0.017	0.007
COV (%)	2.948	1.742	0.727

TABLE 2 Random Variation of Measured COMAC (First Data Set as Reference)

Pt #	MEAN	STD	COV (%)	Pt #	MEAN	STD	COV (%)
1	0.837	0.077	9.156	28	0.955	0.048	4.986
2	0.955	0.030	3.177	29	0.921	0.056	6.045
3	0.992	0.006	0.571	30	0.870	0.158	18.178
4	0.994	0.007	0.720	31	0.917	0.115	12.535
5	0.996	0.003	0.300	32	0.984	0.013	1.295
6	0.992	0.009	0.889	33	0.995	0.006	0.629
7	0.997	0.002	0.240	34	0.997	0.003	0.337
8	0.997	0.003	0.332	35	0.995	0.007	0.713
9	0.988	0.012	1.168	36	0.996	0.004	0.367
10	0.996	0.004	0.424	37	0.992	0.010	0.971
11	0.991	0.010	1.040	38	0.986	0.012	1.175
12	0.981	0.020	2.069	39	0.861	0.045	5.188
13	0.988	0.009	0.959	40	0.982	0.010	1.003
14	0.877	0.055	6.289	41	0.996	0.004	0.430
15	0.670	0.213	31.840	42	0.997	0.001	0.137
16	0.902	0.095	10.571	43	0.993	0.005	0.517
17	0.966	0.042	4.368	44	0.987	0.007	0.666
18	0.984	0.011	1.153	45	0.994	0.004	0.395
19	0.994	0.005	0.497	46	0.869	0.066	7.545
20	0.987	0.020	1.999	47	0.944	0.049	5.163
21	0.996	0.008	0.789	48	0.995	0.004	0.360
22	0.969	0.004	0.385	49	0.996	0.003	0.320
23	0.973	0.013	1.357	50	0.998	0.003	0.254
24	0.996	0.003	0.343	51	0.996	0.006	0.584
25	0.973	0.025	2.551	52	0.997	0.006	0.579
26	0.981	0.020	1.997	53	0.998	0.002	0.215
27	0.970	0.024	2.460	54	0.926	0.084	9.073

As seen from the results in Table 1, the maximum standard deviation and COV were 0.086 Hz and 0.0034, respectively. These random changes appeared to be insignificant for identifying the corresponding frequencies. The obtained damping ratios showed much more significant variation, highlighted by the maximum COV of 0.0992. This can be attributed mainly to the very low damping typically observed in steel structures. In general, measuring low damping reliably is difficult.

No significant changes in the mode shapes were observed during these consecutive tests. Figure 5 shows the variation of a typical mode for Girder 1 by solid lines. Their derivatives, MAC and COMAC, are given in Tables 1 and 2. The maximum standard deviation in MAC was 0.025 for Mode 1. The maximum COV of MAC was 0.0295, and the maximum COV in COMAC was 0.0629, excluding data points at supports (Points 1, 15, 16, 30, 31, 38, 39, 46, 47, and 54). These points showed little movement, resulting in high noise-to-signal ratios. COMAC values at these points thus were not reliable, showing high COV values. COV values in Tables 1 and 2 generally show less significant variations in MAC and COMAC than in the damping ratios. On the other hand, they were more significant than those in the modal frequencies. This is because the MAC and COMAC values were defined and calculated from the

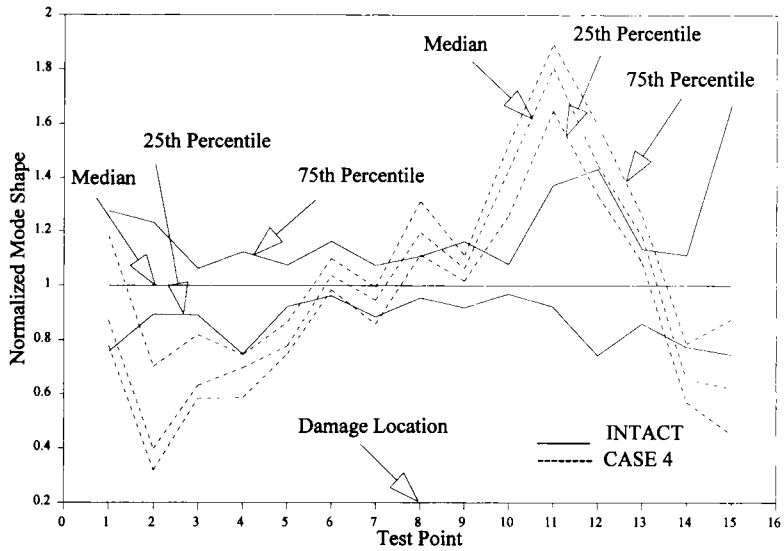

Note: All mode shapes are normalized by the median mode shape at intact.

FIGURE 5 Variation in Mode 1 due to damage Case 4 (all mode shapes are normalized by the median mode shape when intact).

mode shapes, which were in turn determined using the modal frequencies.

These results indicate that frequencies, mode shapes, and MAC and COMAC values can be estimated with relatively higher consistency than damping ratios. This is also in agreement with the test results obtained from earlier laboratory tests (*9*). Hence, it was decided that they were to be used as candidates for fundamental structural signatures. Their sensitivity to damage was a focus of this study. The results indicate that structural damage will not be detectable if it results in less deviation in modal parameters than the corresponding random variation.

Test Program

Modal testing was conducted on the test bridge to confirm the results obtained in the laboratory (*9*) and to gain field experience. Three simulated damage scenarios were introduced by a sawcut 1.6 mm wide:

- Scenario 1: Flange cracking at midspan.
- Scenario 2: Flange cracking at one-third span.
- Scenario 3: Web cracking at midspan.

Table 3 gives more details of the damage cases. These simulated damages were introduced progressively in steps as indicated there. At least three modal tests were conducted for each case, except for Case 2, which included only one test. These data were obtained at temperatures above freezing. Note that these simulated damage cases are more severe than fatigue cracks visible during actual inspection, which were simulated in the earlier laboratory study (*9*). The intention was to examine whether the earlier conclusions would be valid for cases of more critical damage.

Results and Discussion

The first three modes of the field bridge were used in analyzing data for damage diagnosis. Measured modal frequencies, mode shapes, MAC, and COMAC are discussed here. Mean modal frequencies for each damage case are given in Table 4. Corresponding mean MAC and COMAC values (calculated with the first set of test data as reference) were also estimated accordingly for each damage case, as shown in Tables 5 and 6, respectively. These mean values are not adequate for damage diagnosis because of the random variation observed. For example, Table 4 shows the mean of the second modal frequency increasing and decreasing for Cases 3 and 4, although damage severity increased monotonically. These results also indicate that mean frequencies generally decrease with damage (as stiffness of the structure decreases), with several exceptions. Statistical techniques were then used to analyze the data obtained, and results are discussed in the following paragraphs.

Analysis of variance (ANOVA) was performed using the Tukey range method to estimate 95 percent confidence intervals for the means of modal frequencies for all damage cases (*12*). In other words, the mean values of another sample for modal frequencies will be within

TABLE 3 Damage Scenarios and Test Program

Scenario	Case	CRACK DETAILS			No. of repeated tests
		Location*	Length, l (mm)	Depth, d (mm)	
1	1	G1, MS, Point 23	207.65 (FFW)	8.71 (HFT)	4
1	2	G1, MS, Point 23	207.65 (FFW)	17.42 (FFT)	1
1	3	G2, MS, Point 8	207.65 (FFW)	8.71 (HFT)	3
1	4	G2, MS, Point 8	207.65 (FFW)	17.42 (FFT)	10
2	5	G1 & G2, 1/3S, Points 5 & 20	207.65 (FFW)	8.71 (HFT)	3
2	6	G1 & G2, 1/3S, Point 5 & 20	207.65 (FFW)	17.42 (FFT)	3
3	7	G1 & G2, MS, Points 8 & 23	10.24 (FWT)	152.40 (HWD)	3

* MS = Midspan, 1/3S = One-Third Span, FFW = Full Flange Width, FWT = Full Web Thickness, HFT = Half Flange Thickness, FFT = Full Flange Thickness, and HWD = Half Web Depth.

these intervals with a probability of 95 percent. All modal tests were performed in a temperature range of 3.9 to 27.2°C. The confidence intervals were first estimated by assuming both temperature and simulated damage as influencing factors and adjusting the means with temperature effects filtered. Typical results for Mode 1 are given in Table 7. The confidence intervals were estimated again with the simulated damage as the only influencing variable (i.e., assuming no influence of temperature). These results for Mode 1 are given in Table 8. Comparison of Tables 7 and 8 indicates that these results are virtually the same. Results for other modes showed similar behavior. It was thus concluded that, for practical purposes, temperature had no significant effect.

Results given in Table 4 also indicate a tendency of frequency shift with progressive damage cases. The two-sample *t*-test was used to quantify this tendency (*12*). This statistical analysis tests the hypothesis if the mean values of two populations are identical, using the two mode shapes (before and after damage) of respective

TABLE 4 Mean Modal Frequencies for Intact and Damage Cases

Case	Mode		
	1	2	3
int	10.90	20.21	36.79
1	10.57	20.23	36.67
2	10.78	20.15	36.70
3	10.63	20.31	37.16
4	10.00	19.69	35.24
5	10.07	19.64	35.30
6	9.94	19.63	34.89
7	9.49	18.56	34.01

TABLE 5 Mean MAC for Intact and Damage Cases (First Data Set as Reference)

Case	Mode		
	1	2	3
intact	0.848	0.976	0.963
1	0.838	0.987	0.964
2	0.866	0.967	0.957
3	0.829	0.965	0.940
4	0.829	0.967	0.936
5	0.852	0.980	0.942
6	0.862	0.975	0.941
7	0.818	0.975	0.901

TABLE 6 Mean COMAC for Intact and Damage Cases (First Data Set of Impact Case as Reference)

Pt #	CASE							
	intact	1	2	3	4	5	6	7
1	0.837	0.969	0.759	0.809	0.800	0.891	0.908	0.942
2	0.955	0.914	0.927	0.975	0.891	0.853	0.920	0.706
3	0.992	0.976	0.993	0.988	0.991	0.992	0.976	0.980
4	0.994	0.995	0.986	0.986	0.989	0.990	0.989	0.988
5	0.996	0.983	0.997	0.992	0.995	0.995	0.997	0.992
6	0.992	0.996	0.989	0.989	0.993	0.987	0.989	0.995
7	0.997	0.986	0.998	0.996	0.996	0.995	0.997	0.993
8	0.997	0.995	0.994	0.993	0.992	0.987	0.994	0.993
9	0.988	0.995	0.991	0.974	0.983	0.971	0.972	0.977
10	0.996	0.991	0.979	0.978	0.983	0.964	0.974	0.974
11	0.991	0.977	0.969	0.957	0.958	0.949	0.967	0.946
12	0.981	0.982	0.945	0.966	0.960	0.956	0.961	0.968
13	0.988	0.982	0.992	0.983	0.977	0.984	0.986	0.972
14	0.877	0.792	0.938	0.919	0.907	0.889	0.941	0.917
15	0.670	0.787	0.983	0.440	0.906	0.821	0.949	0.796
16	0.902	0.831	0.851	0.922	0.864	0.832	0.903	0.845
17	0.966	0.978	0.995	0.977	0.945	0.928	0.915	0.937
18	0.984	0.975	0.997	0.991	0.977	0.982	0.963	0.981
19	0.994	0.984	0.983	0.987	0.979	0.971	0.970	0.972
20	0.987	0.986	0.993	0.998	0.993	0.993	0.985	0.996
21	0.996	0.997	0.999	0.997	0.996	0.998	0.998	0.995
22	0.969	0.951	0.971	0.969	0.941	0.947	0.936	0.937
23	0.973	0.988	0.999	0.997	0.995	0.995	0.995	0.991
24	0.996	0.990	0.999	0.999	0.996	0.997	0.994	0.997
25	0.973	0.985	1.000	0.996	0.967	0.976	0.979	0.995
26	0.981	0.977	0.975	0.947	0.984	0.970	0.980	0.949
27	0.970	0.960	0.985	0.997	0.902	0.962	0.991	0.937
28	0.955	0.963	0.978	0.919	0.869	0.968	0.965	0.931
29	0.921	0.808	0.714	0.746	0.780	0.927	0.859	0.710
30	0.870	0.968	0.989	0.973	0.921	0.973	0.956	0.963
31	0.917	0.895	0.620	0.715	0.717	0.676	0.768	0.906
32	0.984	0.972	0.978	0.989	0.986	0.994	0.949	0.977
33	0.995	0.995	0.992	0.998	0.996	0.999	0.991	0.994

(continued on next page)

TABLE 6 (*continued*)

34	0.997	0.995	0.999	0.993	0.996	0.999	0.995	0.996
35	0.995	0.993	0.999	0.999	0.997	0.998	0.991	0.983
36	0.996	0.993	0.997	0.994	0.977	0.978	0.983	0.973
37	0.992	0.980	1.000	0.981	0.951	0.975	0.985	0.990
38	0.986	0.947	0.840	0.991	0.978	0.988	0.961	0.672
39	0.861	0.869	0.915	0.827	0.883	0.884	0.798	0.850
40	0.982	0.988	0.987	0.996	0.955	0.971	0.948	0.984
41	0.996	0.998	0.999	0.998	0.981	0.993	0.982	0.995
42	0.997	0.998	1.000	0.996	0.993	0.998	0.998	0.999
43	0.993	0.994	1.000	0.997	0.993	0.993	0.994	0.998
44	0.987	0.991	0.994	0.993	0.977	0.984	0.977	0.999
45	0.994	0.993	0.991	0.993	0.969	0.972	0.964	0.983
46	0.869	0.817	0.963	0.921	0.807	0.936	0.894	0.900
47	0.944	0.937	0.841	0.882	0.896	0.801	0.853	0.734
48	0.995	0.990	0.975	0.992	0.992	0.993	0.996	0.994
49	0.996	0.992	0.989	0.994	0.994	0.994	0.996	0.999
50	0.998	0.997	0.996	0.996	0.992	0.998	0.995	0.998
51	0.996	0.998	0.999	0.997	0.994	0.995	0.997	0.996
52	0.997	0.998	0.996	0.998	0.993	0.990	0.995	0.985
53	0.998	0.989	0.931	0.974	0.979	0.977	0.962	0.978
54	0.926	0.945	0.935	0.978	0.954	0.942	0.993	0.826

TABLE 7 ANOVA Assuming Temperature and Simulated Cracks To Be Effective (with Temperature Effect Filtered)

Damage Case	95% Confidence interval for Mean	
	Lower (Hz)	Upper (Hz)
intact	10.845894	10.944106
1	10.487356	10.642644
2	10.620712	10.931288
3	10.516195	10.735805
4	9.950594	10.048806
5	9.979011	10.158322
6	9.854344	10.033656
7	9.399344	9.578656

TABLE 8 ANOVA Assuming Only Simulated Cracks To Be Effective

Damage Case	95% Confidence interval for Mean	
	Lower (Hz)	Upper (Hz)
INTACT	10.845200	10.944800
1	10.486259	10.643741
2	10.618518	10.933482
3	10.514643	10.737357
4	9.949900	10.049500
5	9.977744	10.159589
6	9.853078	10.034922
7	9.398078	9.579922

populations. Because of the uncertainty inherent in the problem, the test gives the result associated with a probability, which is interpreted here as probability of damage or detectability for damage. Table 9 gives results of the detectability for all the damage cases with reference to the intact condition, except for Case 2, which had only one measured data point and thus was not eligible for the statistical analysis. Except for Modes 2 and 3 under Case 1 and Mode 1 under Case 3, damage detectabilities are higher than 95 percent for all damage cases and all modes, indicating that most of the simulated damage can be detected with high confidence. Table 10 shows damage detectability using MAC values for all damage cases. Most of these detectabilities are lower than those for frequencies in Table 9, indicating lower sensitivity of MAC to damage for this bridge. However, they still can be used to supplement diagnostic decisions. For example, Case 1 damage would not be diagnosed using only the modal frequencies in Table 9, because only one mode showed high damage probability. Supplemented by Table 10 using MAC, this diagnosis can be made with higher confidence because an additional mode (Mode 2) shows a higher damage probability of 92.5 percent. This example has also shown that a limited number of modes may be inadequate for damage diagnosis with higher confidence, either because certain modes are not significantly affected by the damage or because random variation in obtained data is too high; both cases result in difficulty of diagnosis based on a limited number of modes.

Because modal frequencies and MAC refer to individual modes of vibration, diagnosis using these structural signatures can only indicate whether damage or deterioration exists. In practice, when this question is answered positively, the often-needed next step is to identify where the damage is, or at least in which area it has occurred. Without this information, the diagnosis may be considered incomplete. Mode shapes and their derivatives (e.g., COMAC) as structural signatures are natural choices for this purpose because they provide information on vibration patterns for individual points in structures.

TABLE 9 Percentage of Damage Detectability Using Modal Frequencies

Mode	Damage Case w.r.t. Intact					
	1	3	4	5	6	7
1	100	85.2	100	99.3	100	100
2	37.3	98.1	100	100	100	100
3	53.0	99.0	100	96.7	100	100

Note: Detectability was not estimated for Case 2, as only one test was conducted.

TABLE 10 Percentage of Damage Detectability Using MAC

Mode	Damage Case w.r.t. Intact					
	1	3	4	5	6	7
1	37.6	96.2	67.2	10.8	80.7	90.8
2	92.5	73.5	59.9	52.6	5.2	5.4
3	0.5	68.8	99.5	100	97.8	100

Note: Detectability was not estimated for Case 2, as only one test was conducted.

Table 11 presents damage detectability using COMAC by the two-sample *t*-test. Note that the detectabilities in Table 11 refer to the intact condition for all damage cases. The shaded cells indicate the damage locations for each case. For example, Column 1 of Row 5 shows the probability of Point 5 being a damage location due to damage in Case 1. If a 95 percent confidence in diagnosis is required, Points 1, 7, 14, 23, 48, and 49 will be identified as damage locations, simply because they all have damage probabilities of more than 95 percent. Even if Point 1 is excluded because of its location at a support, the rest still do not definitely lead to the correct damage location (i.e., Point 23). Using the same criterion, damage detectabilities for Case 3 show Points 4, 15, 23, 25, 27, 40, and 44 as the damage locations, failing to simultaneously identify Points 8 and 23. Further, Case 7 includes damage locations as Points 5, 8, 20, and 23. The same damage location identification criterion will lead to 11 points being identified as damage locations, with three actual damage locations missing.

Table 12 shows damage detectability by the two-sample *t*-test for four arbitrarily selected locations and four actual damage locations, directly using mode shapes. The shaded cells indicate actual damage locations for the respective damage cases. Unfortunately, they do not always show highest detectabilities. In other words, other points will be falsely identified as damage locations if the real damage locations are identified. Note that this was also observed when all data points were included in the analysis. These results indicate that mode shapes were affected comparably at points beyond and within the damage vicinity.

This situation can be illustrated more intuitively using the results shown in Figure 5. For a damage Case 4 at Points 8 and 23 (midspan of girders), it shows the variation of Mode 1 of Girder 1 at intact and after dam-

TABLE 11 Percentage of Damage Detectability Using COMAC

Mode	Damage Case w.r.t. Intact						Mode	Damage Case w.r.t. Intact					
	1	3	4	5	6	7		1	3	4	5	6	7
1	99.9	32.6	63.4	84.7	94.8	96.9	30	88.0	89.7	56.1	89.6	83.4	83.4
2	72.6	56.0	90.9	62.6	58.8	100	31	27.6	57.1	98.4	68.7	74.4	17.9
3	88.5	36.8	7.1	2.2	46.8	88.0	32	54.1	69.9	21.0	92.5	79.4	83.0
4	26.1	98.1	70.6	58.2	31.0	61.0	33	10.5	60.0	30.7	86.1	68.4	27.6
5	90.9	40.3	70.6				34	52.4	56.7	44.7	71.7	49.7	44.4
6	78.3	15.2	25.8	56.6	39.3	52.5	35	31.4	90.1	65.1	80.1	35.5	63.3
7	99.4	16.3	25.9	39.9	1.8	95.1	36	56.7	42.4	100	95.1	97.9	99.5
8	34.8						37	81.6	57.2	81.2	73.0	57.7	37.1
9	79.6	85.1	66.1	99.1	84.0	72.3	38	53.8	74.7	78.8	28.2	65.1	61.4
10	40.9	85.7	99.1	96.6	96.7	87.2	39	15.7	26.4	57.1	59.3	40.9	21.5
11	83.0	90.9	100	88.5	90.1	93.7	40	70.7	99.6	98.5	55.7	100	35.5
12	1.6	53.6	96.9	91.0	96.1	80.9	41	55.6	80.8	100	52.9	99.9	16.1
13	51.0	65.6	97.1	50.1	28.7	82.5	42	61.3	23.7	59.0	43.0	83.8	91.1
14	95.7	80.8	79.5	24.0	96.3	86.3	43	31.3	58.0	14.1	5.9	4.6	97.3
15	69.4	96.8	98.6	69.1	99.3	66.3	44	78.8	97.1	97.3	25.4	85.3	99.9
16	57.6	28.6	65.0	52.7	0.7	33.4	45	35.3	14.5	100	77.8	99.6	98.6
17	46.0	43.0	78.8	64.5	97.0	59.9	46	58.1	88.9	74.3	90.0	36.0	55.2
18	26.1	49.4	73.8	16.2	82.8	38.4	47	24.1	54.0	96.2	87.8	100	90.6
19	72.6	47.9	99.6	79.8	83.1	90.6	48	99.5	58.1	76.8	45.4	59.8	8.9
20	10.2	83.0	52.8				49	95.2	86.9	61.4	50.3	9.2	96.5
21	34.6	16.0	10.1	58.7	53.5	9.8	50	30.3	58.8	75.4	43.6	50.5	16.2
22	87.7	3.2	100	97.9	92.7	98.3	51	76.5	55.5	29.5	33.0	56.5	7.3
23							52	4.8	24.1	90.4	90.5	55.5	97.4
24	83.9	83.0	4.9	14.4	38.9	33.7	53	76.6	77.0	99.9	100	91.9	96.7
25	61.3	97.4	36.4	13.0	37.3	96.4	54	40.5	88.0	54.9	39.5	94.8	83.7
26	23.0	36.9	24.4	51.6	6.1	94.3							
27	40.5	98.8	89.7	25.4	96.5	40.7							
28	27.6	35.8	94.1	40.9	33.8	56.1							
29	86.6	54.0	94.9	7.3	40.8	67.3							

Note: Detectability was not estimated for Case 2, as only one test was conducted. Shaded cells indicate damage locations.

TABLE 12 Percentage of Damage Detectability Using Mode Shapes

Mode 1	Damage Case w.r.t. Intact					
Pt #	1	3	4	5	6	7
5	99.8	93.9	98.9			
8	48.2					
11	76.8	94.5	100.0	91.1	95.0	96.6
20	20.1	75.1	16.7			
23						
26	39.2	26.7	49.5	80.5	38.7	99.7
33	64.5	75.5	100.0	98.8	97.9	80.4
52	90.4	27.0	56.9	75.9	48.1	21.9

Mode 2	Damage Case w.r.t. Intact					
Pt #	1	3	4	5	6	7
5	1.1	59.1	81.8			
8	48.1					
11	89.9	82.5	89.5	84.6	92.0	95.2
20	6.5	86.4	68.0			
23						
26	12.0	86.0	47.0	27.6	49.4	86.2
33	96.6	80.5	100.0	100.0	100.0	98.4
52	94.3	26.3	88.7	97.4	98.2	78.9

Mode 3	Damage Case w.r.t. Intact					
Pt #	1	3	4	5	6	7
5	65.2	81.2	96.3			
8	42.2					
11	27.4	29.3	97.3	88.4	91.1	100.0
20	30.5	18.0	98.7			
23						
26	92.9	90.8	42.3	5.9	36.0	99.6
33	99.9	1.9	100.0	99.5	100.0	54.4
52	38.0	69.6	88.5	84.5	7.3	98.9

Note: Shaded cells indicate damage locations.

age, described by the median, 25th-percentile, and 75th-percentile values. For clarity, these values are normalized by the median mode shape of the intact structure. Note that Point 23 is transversely at the same location as Point 8 but on the other girder (Figure 2). It can be seen that the mode shape changed at all locations along the girder (including damage location); Points 2 and 11 changed the most, being 2.9 and 1.45 m away from the damage location points.

Using mode shapes or their derivatives for identifying the location of damage is essentially based on an assumption that local damage will change mode shapes at or near the damage location more significantly than in other areas. Figure 5 shows that this assumption is

not verified and instead demonstrates proportional changes of the mode shapes at various locations. This happens because upon local damage, adjacent structural elements autogenously distribute load effects through an altered load path system, and local damage effects are thus distributed to other elements of the structure. This self-adjustment capability is believed to have been provided by intentional and unintentional redundancy.

The preceding results also confirm the findings from the earlier laboratory tests (*9*). It should be noted that these consistent findings are associated with the specific test instrumentation used. They may indicate the need to improve instrumentation by reducing measurement noise and attaining more extensive simultaneous coverage over the structure.

Conclusions

Modal frequencies may be used to detect the existence of damage or deterioration simulated here for highway bridges. Cross-diagnosis using multiple signatures such as mode shapes, MAC, and COMAC is warranted for such detection, because a single signature may not be conclusive due to inevitable variation of measured data. Criteria for warning triggering that use these signatures need to be determined by taking into account their random variation affecting sensitivity of detection. However, damage locations cannot be identified using mode shapes and their derivatives, because damage affects mode shapes comparably at all damaged and undamaged locations. For complete damage diagnosis, including existence and location, improved instrumentation may be needed for lower noise and more extensive simultaneous coverage.

ACKNOWLEDGMENTS

This project was partially supported by the U.S. Department of Transportation. Many New York State Department of Transportation personnel contributed to make this study possible, and their efforts are deeply appreciated.

REFERENCES

1. FHWA, U.S. Department of Transportation. National Bridge Inspection Standards: Frequency of Inspection and Inventory. *Federal Register*, Vol. 52, No. 66, April 7, 1987.
2. R. I. Shores Cracked Viaduct. *Engineering News-Record*, Feb. 4, 1988, pp. 20–28.
3. Collapse of New York Thruway (I-90) Bridge over the Schoharie Creek near Amsterdam, New York, April 5, 1987. Report PB 88-916202, NTSB/HAR-88/02. *Highways Accident Report*, National Transportation Safety Board, 1988.
4. Ewins, D. J. *Modal Testing: Theory and Practice*. John Wiley, New York, 1984.
5. Mazurek, D. F., and J. T. DeWolf. Experimental Study of Bridge Monitoring Technique. *Journal of Structural Engineering*, ASCE, Vol. 116, No. 9, Sept. 1990, pp. 2532–2549.
6. Pandey, A. K., M. Biswas, and M. M. Samman. Damage Detection from Changes in Curvature Mode Shapes. *Journal of Sound and Vibration*, Vol. 145, No. 2, March 1991.
7. Wolf, T., and M. Richardson. Fault Detection in Structures from Changes in the Modal Parameters. *Proc., 7th International Modal Analysis Conference*, Las Vegas, Nev., Jan. 1989, pp. 87–94.
8. Hearn, G., and R. B. Testa. Modal Analysis for Damage Detection in Structures. *Journal of Structural Engineering*, ASCE, Vol. 117, No. 10, Oct. 1991, pp. 3042–3063.
9. Alampalli, S., G. Fu, and E. W. Dillon. Measured Bridge Vibration for Damage Detection. Final report. New York State Department of Transportation, Albany (in preparation).
10. Allemang, R. J., and D. L. Brown. A Correlation Coefficient for Modal Vector Analysis. *Proc., 1st International Modal Analysis Conference*, Bethel, Conn., 1982, pp. 110–116.
11. Lieven, N. A. J., and D. J. Ewins. Spatial Correlation of Mode Shapes, The Coordinate Modal Assurance Criterion (COMAC). *Proc., 6th International Modal Analysis Conference*, Kissimmee, Fla., Feb. 1988, pp. 690–695.
12. Box, G. E. P., W. G. Hunter, and J. S. Hunter. *Statistics for Experiments*. John Wiley & Sons, New York, 1978.